RESTORE: Robust Estimation of Tensors by Outlier Rejection

Lin-Ching Chang,[1] Derek K. Jones,[1,2] and Carlo Pierpaoli[1]*

Signal variability in diffusion weighted imaging (DWI) is influenced by both thermal noise and spatially and temporally varying artifacts such as subject motion and cardiac pulsation. In this paper, the effects of DWI artifacts on estimated tensor values, such as trace and fractional anisotropy, are analyzed using Monte Carlo simulations. A novel approach for robust diffusion tensor estimation, called RESTORE (for robust estimation of tensors by outlier rejection), is proposed. This method uses iteratively reweighted least-squares regression to identify potential outliers and subsequently exclude them. Results from both simulated and clinical diffusion data sets indicate that the RESTORE method improves tensor estimation compared to the commonly used linear and nonlinear least-squares tensor fitting methods and a recently proposed method based on the Geman–McClure M-estimator. The RESTORE method could potentially remove the need for cardiac gating in DWI acquisitions and should be applicable to other MR imaging techniques that use univariate or multivariate regression to fit MRI data to a model. Magn Reson Med 53:1088–1095, 2005. Published 2005 Wiley-Liss, Inc.†

Key words: robust estimation; outliers; trace; anisotropy; diffusion; tensor

Diffusion tensor magnetic resonance imaging (DT-MRI) is used increasingly in clinical research for its ability to depict white matter tracts and for its sensitivity to microstructural and architectural features of brain tissue. Diffusion tensor maps are typically computed by fitting the signal intensities from diffusion weighted images as a function of their corresponding *b*-matrices (1) according to the multivariate least-squares regression model proposed by Basser et al. (2). The least-squares (LS) regression model takes into account the signal variability produced by thermal noise by including the assumed signal variance as a weighting factor in the tensor fitting. Signal variability in diffusion weighted imaging (DWI), however, is influenced not only by thermal noise but also by spatially and temporally varying artifacts. Such artifacts originate from the so called "physiologic noise" such as subject motion and cardiac pulsation, as well as from acquisition-related factors such as system instabilities. The multivariate least-squares regression model assumes that the signal variability in the DWI is affected only by thermal noise and does not account for signal perturbations and potential outliers that originate from artifacts. While the signal variability produced by thermal noise is approximately Gaussian distributed (3), signal variability produced by physiologic noise and other artifacts does not have a known parametric distribution and currently cannot be modeled. Situations in which experimental errors do not follow a Gaussian distribution, or are unknown, are generally addressed statistically by using "robust" estimators, which are less sensitive to the presence of outliers.

Surprisingly, the use of robust estimators has been largely neglected by the DT-MRI community. We are aware of only one robust tensor estimation approach recently proposed by Mangin et al. (4), which is based on the well-known Geman-McClure M-estimator (5) (we will refer to Mangin's approach as GMM in this paper). This approach uses an iteratively reweighted least-squares fitting in which the weight of each data point is set to a function of the residuals of the previous iteration. The GMM method ensures that potentially artifactual data points having large residuals are given lower weights in the estimation of the tensor parameters. Clearly, this approach is statistically more robust than the standard LS methods in the presence of outliers. However, by using the residuals as the only determinants of the weights, it discards the information contained in the known distribution of errors related to thermal noise.

In this paper, we propose an alternative approach, called robust estimation of tensors by outlier rejection (RESTORE), which uses an iteratively reweighted LS regression, such as the GMM method, only to identify potential outliers,which are then excluded. The final fit is performed with the remaining data points using the constant weights that appropriately describe the error introduced by Gaussian distributed noise.

We compare the performance of the RESTORE algorithm with that of the GMM method, nonlinear LS fitting, and linear LS fitting using both synthetic data and DT-MRI data acquired from healthy volunteers. In particular we investigate the ability of the RESTORE algorithm to provide reliable tensor estimation in the presence of artifacts resulting from cardiac pulsation.

METHODS

Algorithm

Table 1 lists the fitted equations and their respective weighting functions for three previously proposed diffusion tensor fitting approaches: (i) the widely used linear least-squares fitting of the logarithmically transformed signals (linear LS); (ii) nonlinear least-squares fitting of the signals (nonlinear LS); and (iii) nonlinear LS fitting with robust GMM.

[1]Section on Tissue Biophysics and Biomimetics, Laboratory of Integrative Medicine and Biophysics, National Institute of Child Health and Human Development, National Institutes of Health, Bethesda, Maryland, USA.

[2]Centre for Neuroimaging Sciences, Institute of Psychiatry, London, United Kingdom.

*Correspondence to: Carlo Pierpaoli, National Institutes of Health, Building 13, Room 3W16, 13 South Drive, Bethesda, MD 20892-5772, USA. E-mail: cp1a@nih.gov

Received 9 September 2004; revised 29 November 2004; accepted 29 November 2004.

DOI 10.1002/mrm.20426
Published online in Wiley InterScience (www.interscience.wiley.com).

Table 1
Regression Methods Used in Diffusion Tensor Estimation

Method	Equation	Weighting function
Linear least-squares	$\ln S_{(\mathbf{b})} = \ln S_{(0)} - \mathbf{bD}$	$\omega_i = \frac{(S_{(\mathbf{b})})^2}{\sigma^2}$
Nonlinear least-squares	$S_{(\mathbf{b})} = S_{(0)} * \exp(-\mathbf{bD})$	$\omega_i = \frac{1}{\sigma^2}$
Geman–McClure M-estimator	$S_{(\mathbf{b})} = S_{(0)} * \exp(-\mathbf{bD})$	$\omega_i = \frac{1}{r_i^2 + C^2}$

All methods minimize the value of χ^2 computed from the equation

$$\chi^2 = \sum_i \omega_i \times (y_i - y(x_i))^2 , \quad [1]$$

where y_i is the experimental value of the ith data point, x_i is the value of the independent variable (or regressor) for that data point, $y(x_i)$ is the corresponding fitted value, and ω_i is the weighting factor for the data point.

For all approaches, the independent variable x is the b-matrix (**b**), while the dependent variable y is, respectively, the signal intensity S for the nonlinear LS and GMM models and its natural logarithm for the linear LS model. The diffusion tensor, **D**, and the signal intensity with no diffusion sensitization $S_{(0)}$, or its logarithm $\ln(S_{(0)})$, are the estimated parameters (2). In Table 1, σ is the signal SD, r_i is the residual or difference between the experimental value y_i of the ith data point and its estimated value $y(x_i)$. The scale factor C affects the shape of the GMM weighting function and represents the expected spread of the residuals (i.e., the SD of the residuals) due to Gaussian distributed noise. The scale factor C can be estimated by many robust scale estimators. We used the median absolute deviation (MAD) estimator because it is very robust to outliers having a 50% breakdown point (6,7). The explicit formula for C using the MAD estimator is $C = 1.4826 \times \text{MAD} = 1.4826 \times \text{median}\{|r_1 - \hat{r}|, |r_2 - \hat{r}|, \ldots, |r_n - \hat{r}|\}$, where $\hat{r} = \text{median}\{r_1\, r_2, \ldots, r_n\}$ and n is the number of data points. The multiplicative constant 1.4826 makes this an approximately unbiased estimate of scale when the error model is Gaussian.

A flow chart describing the RESTORE algorithm is shown in Fig. 1. The diffusion tensor is first computed using the nonlinear LS method with constant weights ($w = 1/\sigma^2$) and the result from linear LS fitting as the initial guess of parameters. The linear LS fitting is implemented using the "regress" procedure from IDL, and the nonlinear LS regression is implemented using the MPFIT procedure (8), which is also written in IDL based on the Levenberg–Marquardt algorithm. The expected signal variance σ^2 can be estimated from the variance of the noise measured in a background region of the images according to Henkelman (3), ($\sigma = 1.5267 \times$ (SD of the background noise)). The results of this first fitting are then evaluated against a goodness-of-fit criterion. If the residuals of all data points lie within a given confidence interval, it is assumed that no outliers are present and the results are accepted with no further processing. We set the confidence interval equal to three times the expected SD of the signal. Other goodness of fit criteria can be used, for example, those based on the analysis of χ^2.

If the goodness of fit criterion is not satisfied, an iterative reweighting process using the GMM weighting function is initiated. The weight for each data point is normalized to the average of all the weighting factors to yield the maximum likelihood that the fitting function represents the parent distribution (9). The reweighting process continues iteratively until it satisfies a convergence criterion. When the iterative process is finished, points lying outside a confidence interval (set to three times the expected signal SD) are identified as outliers and excluded. Finally, the remaining data points are weighted equally and the diffusion tensor is recomputed using the nonlinear LS method.

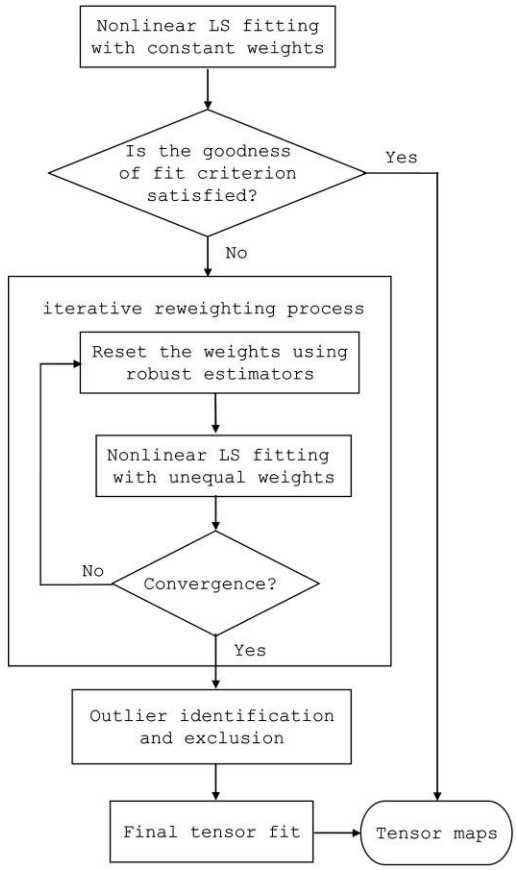

FIG. 1. Flow diagram of the RESTORE algorithm.

Monte Carlo Simulations

We performed Monte Carlo simulations to investigate the effects of artifacts on diffusion tensors estimated with the different fitting methods. We simulated both an isotropic diffusion tensor and a cylindrically symmetric anisotropic diffusion tensor with diffusivity in the x direction set to five times the diffusivity in the y and z directions. The trace of both tensors was set to be representative of the trace of brain parenchyma (2100 $\mu m^2/s$) (10).

Two experimental designs were tested, both with 35 b-values (5 with $b = 0$ and 30 with $b = 1000$ s/mm^2), but with different diffusion sampling direction schemes. The first experimental design was the widely used six diffusion sampling directions scheme (10) (11). This scheme makes an efficient use of the available gradient strength and provides diffusion weighted images with relatively high signal-to-noise ratio per unit time. A recent study by Jones (12), however, showed that the variability of estimated tensor maps can depend on the number of unique gradient sampling orientations and that at least 30 unique sampling orientations are required for rotationally invariant statistical properties of the estimated tensor quantities. Therefore, we also tested a second experimental design with 30 unique sampling directions (13).

For each experimental design and predefined tensor we created synthetic diffusion weighted signal intensity data conforming to the diffusion tensor model. Gaussian distributed noise was then added in quadrature to the synthetic noise-free signal to achieve a signal-to-noise ratio of 25 in the $b = 0$ data. The diffusion tensor was subsequently estimated using: (i) the linear LS; (ii) the nonlinear LS; (iii) the GMM; and (iv) the RESTORE methods from 16384 realizations of these noisy data sets to assess the distribution of tensor values in the absence of artifactual data points.

Artifacts in DWI can cause signal intensities to be lower or higher than their normal values. To simulate these situations, we randomly corrupted some of the $b = 1000$ s/mm^2 data points by either decreasing or increasing their intensity values by 50%. We tested a number of corrupted data points ranging from 1 to 8, i.e., from 3.3 to 26.7% of the 30 $b = 1000$ s/mm^2 signal intensities included in each data set. The distributions of Trace(**D**) and fractional anisotropy (FA) (14) were then computed for the corrupted tensors obtained with all the fitting methods.

Data Corrupted by Cardiac Pulsation Artifacts

Pulsations during the cardiac cycle can cause severe artifacts in diffusion weighted images acquired with no cardiac gating. Such artifacts affect both trace and anisotropy values and are most pronounced in data acquired at specific time points during systole. Previous studies have shown that data acquired at about 120 ms after the onset of the R wave are very prone to corruption by cardiac pulsation (15). In order to assess the performance of the RESTORE method in the presence of cardiac pulsation artifacts, we acquired ECG-gated brain DT-MRI data sets from a healthy volunteer with five different trigger delays after the onset of the R wave. One data set was acquired during the critical systolic period (120-ms delay) and four during the diastolic period when cardiac induced artifacts are less pronounced (320-, 370-, 420-, and 520-ms delay). Images were acquired on a CNV LX 1.5 GE MRI System (General Electric, Milwaukee, WI) with a diffusion weighted, spin-echo, single-shot EPI sequence with $2 \times 2 \times 4$ mm^3 resolution and 42 slices to cover the whole brain. Each data set consisted of 8 replicates of $b = 1100$ s/mm^2 images acquired using the six-direction gradient scheme (10) and 8 $b = 0$ images for a total of 56 images. Prior to the diffusion tensor computation, all images were corrected for eddy current distortion and rigid-body brain motion using the approach of Rohde et al. (16). The diffusion tensor was computed using the linear LS, the nonlinear LS, the GMM, and the RESTORE methods in two sets of pooled data: a "superset" consisting of the four diastolic acquisitions plus the systolic one and a "diastolic set" containing only the four diastolic acquisitions. Our goal was to test which tensor fitting method, once applied to the superset, gave results most similar to those obtained with the diastolic set. Moreover, we wanted to see whether the RESTORE method would identify data points collected during systole (rather than those collected during diastole) as outliers.

RESULTS

Monte Carlo Simulation

When no corrupted data were included, all fitting methods showed similar results. The computed Trace(**D**) had mean values ranging from 2067 to 2077 $\mu m^2/s$ for the linear LS method and 2092 to 2095 $\mu m^2/s$ for the other three methods, which are close to the expected value of 2100 $\mu m^2/s$. The computed FA had mean values ranging from 0.085 to 0.099 for the isotropic case (expected value = 0.000) and 0.769 to 0.772 for the anisotropic case (expected value = 0.770). The discrepancy between computed and expected mean values for the FA in the isotropic case is relatively large, but to be expected considering that noise biases anisotropy indices, particularly for low anisotropy values (17).

Figure 2 shows the effect of outliers on the distributions of Trace(**D**) and FA values computed with the widely used linear LS method. Figure 2a and b shows the case in which artifactual points had their signal intensity decreased by 50%, while Fig. 2c and d shows the case in which artifactual points had their signal intensity increased by 50%. This simulation demonstrates that both Trace(**D**) and FA values are significantly biased by the presence of even a small percentage of outliers. Interestingly, artifacts producing increased signal intensity have a more pronounced effect than artifacts with decreased signal intensity. This finding can be understood by considering that the weighting function used to account for the logarithmic transformation of the data includes the signal intensity squared (see Table 1). With the linear LS method, artifacts reducing the signal intensity also reduce the weights of the corrupted data points in the fitting, thereby reducing their damaging effect on the estimated parameters. This effect is not observed with nonlinear fitting methods in which the weighting function does not contain the signal intensity as a term (data not shown).

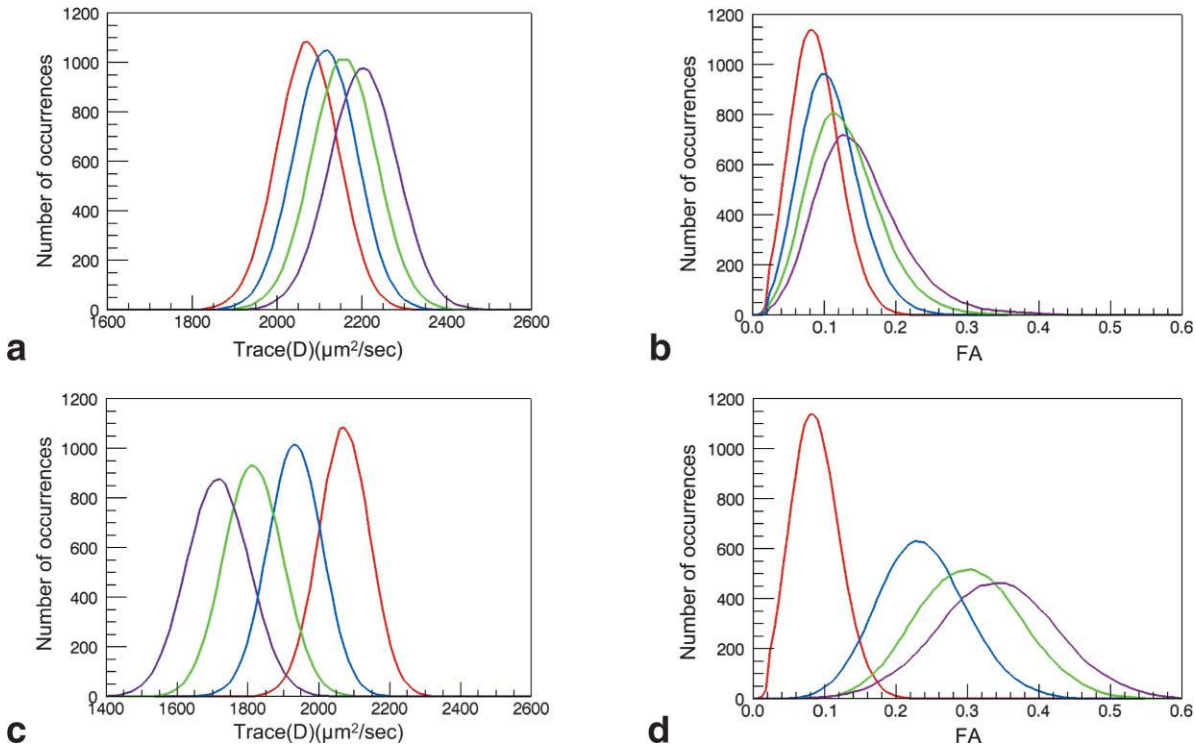

FIG. 2. Trace(**D**) and fractional anisotropy (FA) distributions for an isotropic diffusion tensor obtained from Monte Carlo simulated data using the linear least-squares method. Corrupted data points had intensity decreased by 50% (**a** and **b**) or increased by 50% (**c** and **d**). Different colors represent different percentages of outliers (red = 0%, blue = 6.67%, green = 13.3%, and purple = 20%).

Figure 3 shows the distributions of Trace(**D**) and FA values computed using the three nonlinear fitting approaches: (i) nonlinear LS, (ii) GMM, and (iii) RESTORE. The results of the nonlinear LS fitting are severely affected by the presence of outliers (Fig. 3a and b). The robust GMM approach shows some improvement but, surprisingly, a considerable bias remains (Fig. 3c and d). The RESTORE algorithm is the most robust approach, giving almost unbiased results provided that the number of corrupted point is not excessively high, for example, the blue and red curve are almost superimposed (Fig. 3e and f). When the number of outliers exceeds half of the replications and all outliers occurred in the same direction, the bad points outnumber the good points and both GMM and RESTORE methods fail (e.g., a second hump is observed in the green and purple curves). The results obtained for artifacts that decrease the signal intensity are not shown in the figure but again results from the RESTORE algorithm proved to be the least sensitive to the presence of corrupted data points.

Figure 4 shows the median value of Trace(**D**) as a function of the percentage of corrupted points for the isotropic tensor case. The effect of both signal decreasing (Fig. 4 a) and signal increasing (Fig. 4 b) artifacts using four different methods is shown. The expected value of the median of Trace(**D**) (in the absence of corrupted points) is 2100 $\mu m^2/s$. As the percentage of corrupted points increases, the computed values progressively deviate from the expected values. Computed values from data processed with the RESTORE method show the smallest deviation from the expected values for both signal decreasing and signal increasing artifacts. For a percentage of artifactual data points below 15% the RESTORE method shows virtually no error.

Figure 5 shows a comparison of the distributions of Trace(**D**) and FA values obtained with the RESTORE algorithm for the 6-direction scheme (Fig. 5 a and b) and the 30-direction scheme (Fig. 5c and d). The results for the two schemes are very similar when the percentage of artifactual data points is low (below 10%); however, as the percentage of outliers increases, the 6-direction scheme starts showing a bimodal distribution that is not observed with the 30-direction scheme.

The computation time required for the RESTORE method is acceptable compared to the standard nonlinear LS fitting. If we set the computation time for the nonlinear LS method to 1 in our simulation, the computation time required is 2.53 and 3.51 for GMM and RESTORE, respectively. Given that the results obtained using linear LS and nonlinear LS methods are so similar when no outliers are present in the data, we may use the linear LS for the final tensor fitting to reduce the total computation time. Practically, using the goodness of fit criterion after the initial nonlinear fitting can also reduce the computation time depending on the quality of images.

Data Corrupted by Cardiac Pulsation Artifacts

Previous studies indicate that cardiac-induced artifacts affecting tensor-derived parameters are most pronounced in infratentorial regions of the brain, in particular in the cerebellar peduncles and ventral portions of the cerebel-

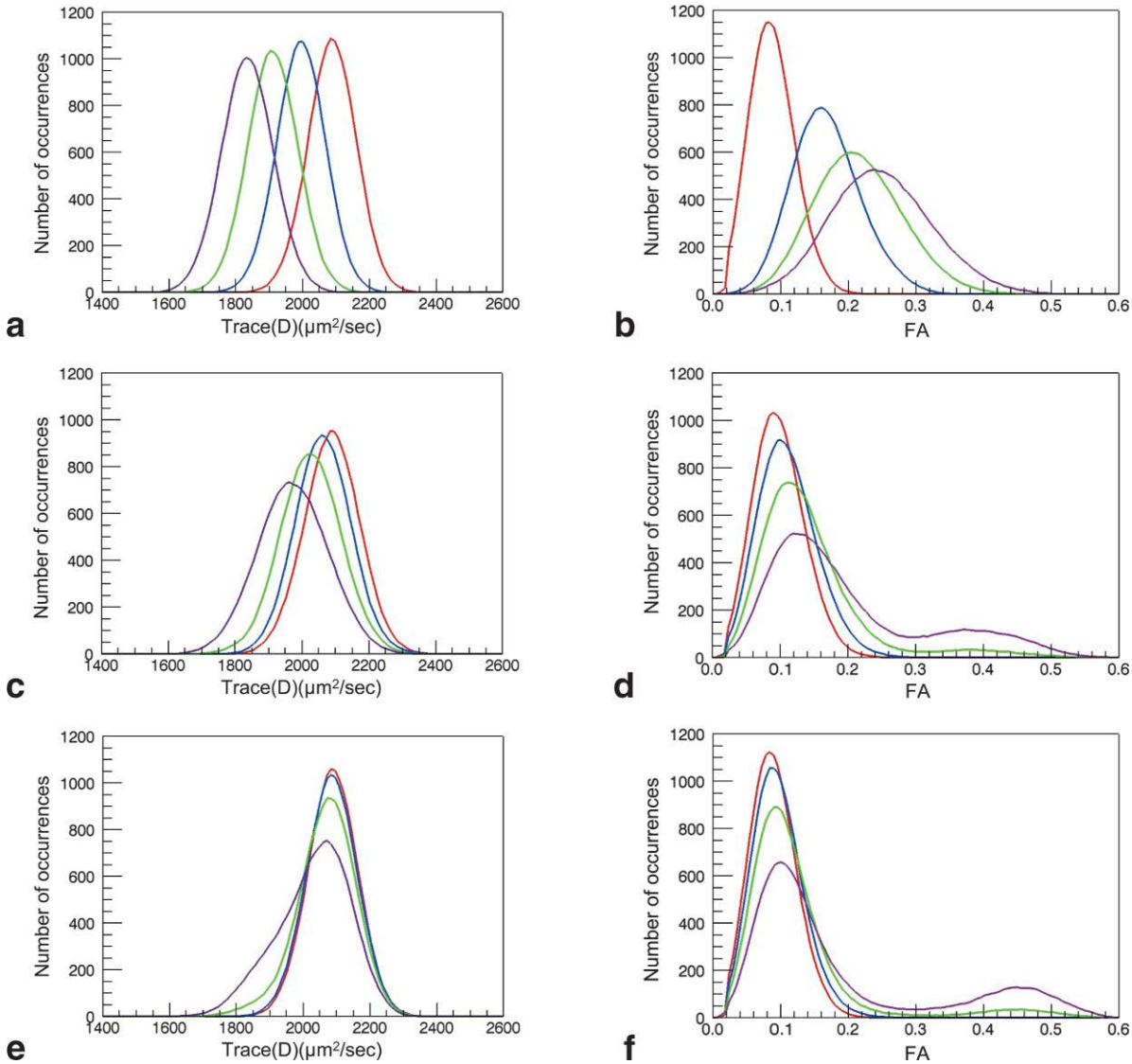

FIG. 3. The Trace(**D**) and fractional anisotropy (FA) distributions for an isotropic diffusion tensor obtained from Monte Carlo simulated data using the nonlinear least-squares method (**a** and **b**), the GMM method (**c** and **d**), and the RESTORE method (**e** and **f**). Corrupted data points had intensity increased by 50%. Different colors represent different percentages of outliers (red = 0%, blue = 6.67%, green = 13.3%,and purple = 20%).

lum (15). We selected a region of interest (ROI) in the ventral portion of the cerebellum and compared the measured values of Trace(**D**) and FA obtained using the superset consisting of the four diastolic acquisitions and one systolic acquisition and the diastolic set containing only the diastolic acquisitions. The average value of Trace(**D**) and FA in the selected ROIs computed with the diastolic dataset using the various fitting approaches was very similar (within 1%). We used the result of the nonlinear LS as a benchmark value for computing the percentage error introduced by the systolic points in the superset according to the formula

$$\text{Percentage error} = 100 \times (\text{value}_{\text{superset}} - \text{value}_{\text{diastole}})/\text{value}_{\text{diastole}}.$$

The percentage error for Trace(**D**) was 9.37% for the nonlinear LS, 2.77% for the GMM, and 1.61% for the RESTORE method. The percentage error for FA was 23.64% for the nonlinear LS, 3.57% for the GMM, and 1.81% for the RESTORE method.

Figure 6 shows that the spatial distribution of outliers identified by the RESTORE method in the superset matches well the regions where cardiac-induced artifacts are known to be most severe. When the RESTORE algorithm is applied to the diastolic set the portion of the image identified as having the highest percentage of outliers is a region suffering from susceptibility artifacts (pointed to by the arrow in Fig. 6b). The cerebellum and brain stem, however, have roughly the same amount of excluded points as the rest of the brain. When the RESTORE algorithm is applied to the superset, the percentage of excluded systolic points is selectively high in the cerebellum and brain stem. These results demonstrate that the RESTORE method successfully excluded the systolic data points from the fitting in areas that are known to be affected by the cardiac pulsation (15).

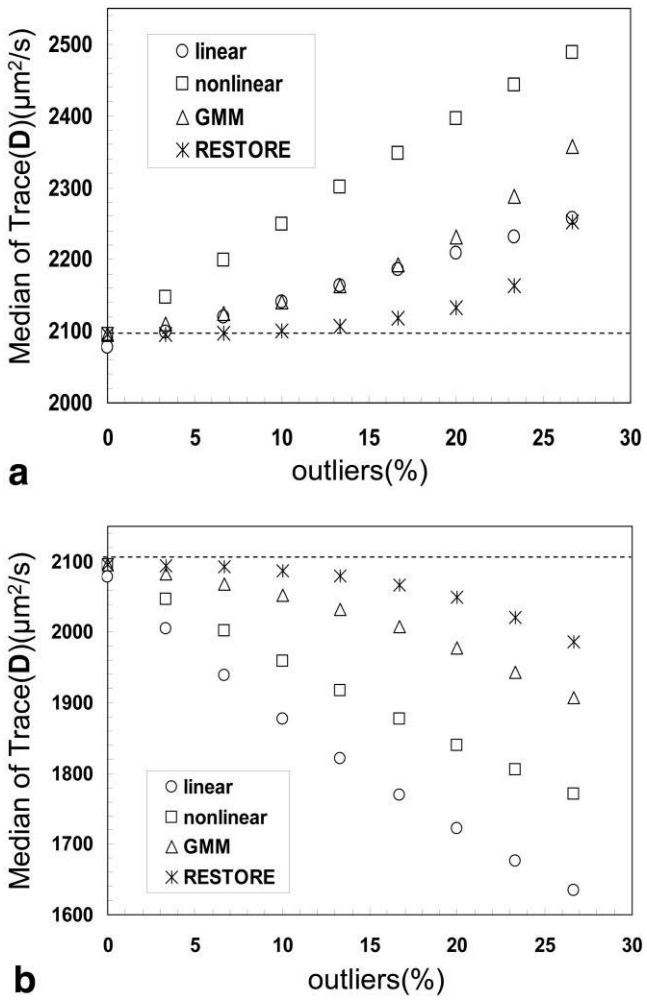

FIG. 4. The median of Trace(**D**) for an isotropic diffusion tensor obtained from Monte Carlo simulated data using different methods. Corrupted data points had intensity decreased by 50% (**a**) or increased by 50% (**b**).

Regarding computation time, processing the superset took less than 2 min using the linear LS method on a Dell 4100 with dual Intel Xeon 2.80-GHz processors. Computation time was 1 hr 56 min for the nonlinear LS method, 2 hr 32 min for the GMM method, and 2 hr 59 min for the RESTORE method.

DISCUSSION

Artifacts are common in clinical DT-MRI acquisitions, especially those originating from cardiac pulsation in ungated acquisitions and those originating from subject motion when scanning uncooperative patients or unsedated pediatric subjects. Signal perturbations produced by such artifacts can be severe and neglecting to account for their contribution can result in erroneous diffusion tensor values. Our Monte Carlo simulations show that a single corrupted data point in the data set can significantly affect the accuracy of the computed diffusion tensor values if tensor computation is performed with the commonly used least-squares regression method. A recently proposed robust tensor fitting approach which utilizes the Geman–McClure M-estimator achieves an improved accuracy of the estimated tensor parameters with respect to both the linear and the nonlinear LS methods in presence of artifacts, but fails to yield completely unbiased results. The proposed RESTORE algorithm proves to be the most robust approach, giving almost unbiased results for both Trace(**D**) and FA provided that the percentage of corrupted points is below 15% (see Fig. 4).

At first glance the significantly improved performance of the RESTORE algorithm compared to that of the GMM method may appear surprising. Outlier diagnostics (e.g., RESTORE) have the same goal as robust regression (e.g., GMM), and in most applications, in which the error distribution is not known a priori, both approaches yield similar results. As we mentioned earlier, our motivation for designing the RESTORE approach was the realization that in diffusion weighted images, even in the presence of artifacts, the error distribution is not completely unknown and that the GMM approach did not make efficient use of the prior information regarding the distribution of errors produced by thermal noise. We believe that the reason for the superior performance of the RESTORE algorithm over the GMM method is essentially related to the more efficient use of such information.

We used the Gema–McClure M-estimator in the iterative reweighting procedure of the RESTORE algorithm for the purpose of providing a direct comparison with the results of a previously proposed robust tensor estimation approach (4). Various types of robust estimators have been successfully used to deal with the presence of outliers such as M-estimators, R-estimators (18), the least median-of-squares, and RANSAC (19). They could replace the Geman–McClure M-estimator in the RESTORE algorithm. The class of M-estimators, however, appears to be one of the more appropriate choices given the underlying Gaussian distribution of errors produced by thermal noise. The scale factor C appearing in the Geman–McClure M-estimator formula (see Table 1) is an estimate of the signal variability due to Gaussian distributed noise. For consistency with the approach previously proposed by Mangin et al. 4, we extracted the value of C from the data by setting it equal to a robust estimate of the SD of the residuals. Alternatively, C can be set equal to the expected signal SD, which can be estimated from measurements of noise in the background of the images. In simulations experiments (that we did not report here), this latter approach showed slightly better performance compared to the case in which data driven estimates of C were used.

Despite the very good performance of the RESTORE algorithm, there are some limitations and opportunities for improvement. The main weakness is of a theoretical nature. The thermal-noise induced errors and the artifact induced errors are intrinsically mixed and we do not attempt to deconvolve them. The artifactual data points that the RESTORE algorithm identifies as outliers (and subsequently eliminates) are those in which the "artifact" error component is large (i.e., outside the bounds of our confidence interval of three standard deviations), but remaining data points that fall within an acceptance confidence interval may also be partially corrupted by artifacts.

Another potential weakness is that the RESTORE method relies on data redundancy, as do other robust

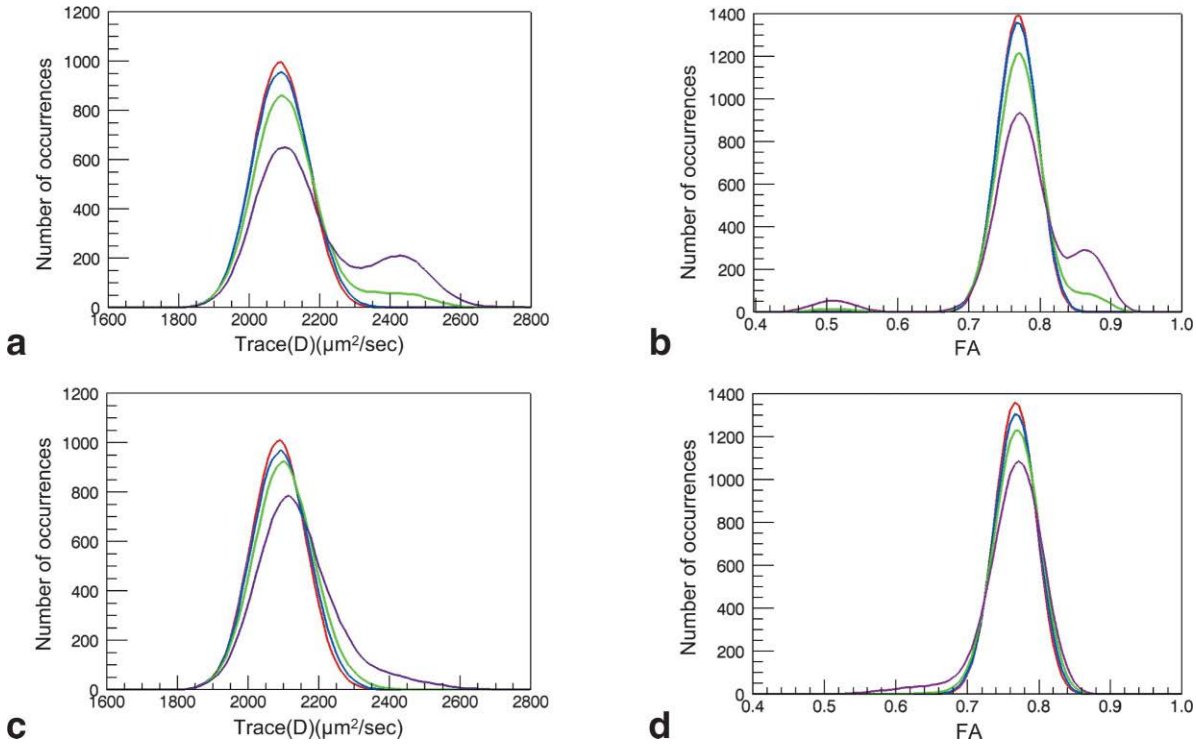

FIG. 5. Comparison of the 6- (**a**) and 30- (**b**) gradient direction schemes showing Trace(**D**) and fractional anisotropy (FA) distributions obtained from Monte Carlo simulated data for an anisotropic diffusion tensor using the RESTORE method. Corrupted data points had intensity decreased by 50%. Different colors represent different percentages of outliers (red = 0%, blue = 6.67%, green = 13.3%, and purple = 20%).

estimation methods. Problems may arise if the data set does not have enough good data points to correctly identify outliers. Interestingly, the percentage of artifactual data points that can be tolerated depends not only on the degree of redundancy of the data set but also on the gradient sampling scheme. In our simulation it was seen that in the 6-direction scheme a bimodal distribution of the computed Trace(**D**) and FA values appeared when there

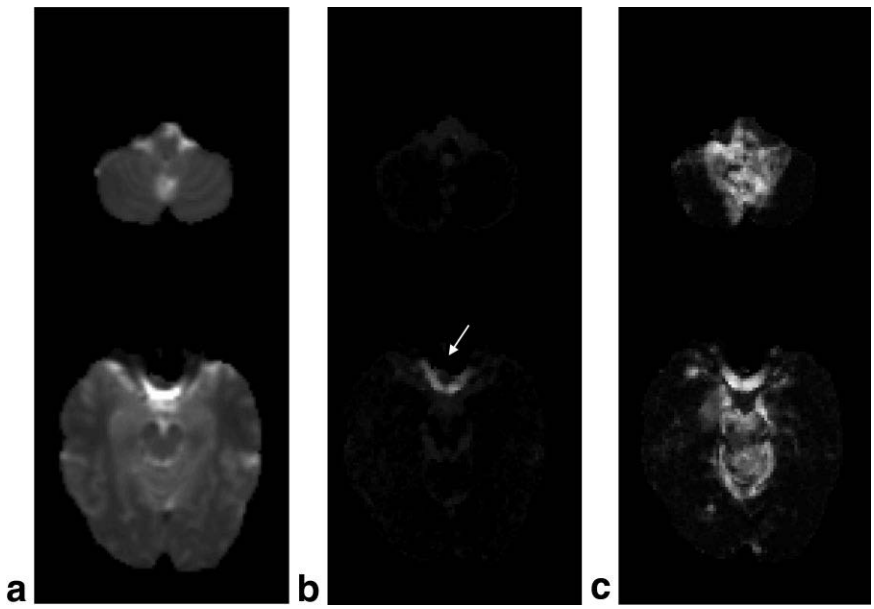

FIG. 6. Maps of the percentage of data points identified as outliers by the RESTORE algorithm in the diastolic data set (**b**) and in the superset (**c**). For the diastolic dataset the map represents the percentage of data points excluded. The arrow in (b) shows the high percentage of outliers is a region suffering from susceptibility artifacts. For the superset the map represents the percentage of systolic data points excluded. Grayscale values range from 0 (black) to 100% (white). The T_2-weighted image is shown in (**a**) for anatomic reference.

were three or more outliers. This effect was not observed with the 30-direction scheme. In the 6-direction scheme there are five replicates per diffusion sampling direction, and when three or more corrupted data points happened to be in the same direction, the good data points were outnumbered by the outliers. In such cases, the outlier diagnostic process fails and the good data points are themselves identified as outliers leading to diffusion tensor parameters with large bias. In the 6-direction scheme there is no redundancy in sampling orientations, and the data points in the remaining 5 directions could not contribute information useful to correctly identify outliers in the direction affected by the corrupted data points. This is not the case with the 30-direction scheme which is relatively immune to this problem because sampling directions are more evenly distributed.

In addition to improving tensor estimation in the simulation, the RESTORE algorithm proved to be very effective in identifying data corrupted by cardiac-induced artifacts in actual DT-MRI data. Cardiac gating lengthens the duration of the scan and it is not routinely performed in clinical DT-MRI. Moreover, some commercially available diffusion weighted imaging sequences perform gating by triggering the acquisition of a series of images collected over several cardiac cycles. With these sequences, only the first image of the series is effectively gated, while the others may still suffer from cardiac-induced artifacts (20). Our results indicate that processing the data with the RESTORE algorithm would be a very effective approach to obtain diffusion tensor parameters immune from cardiac-induced artifacts when data are acquired with ungated or partially gated acquisitions.

In its current implementation, the RESTORE algorithm performs nonlinear fitting of the diffusion weighted data, rather than the much faster linear fitting. Moreover, compared to the conventional nonlinear fitting, the computation time is increased by the iterative reweighting process and the final fitting step after outlier exclusion. Theoretically a linear fitting version of the algorithm can be developed, although designing the proper weighting function for logarithm transformed data corrupted by artifacts may be difficult. Given the length of the processing time, the use of the RESTORE, the GMM, or the nonlinear LS methods may not be feasible for computing diffusion tensor images that need to be displayed "on the fly," during or immediately after the acquisition. However, the problem can be overcome by using parallel processing techniques in a multiprocessor system. The computation time would be reduced in direct proportion to the number of processors available since the tensor fitting is done on a voxel-by-voxel basis.

One possible weakness of nonlinear fitting is its susceptibility to local minima, which may lead to severely flawed estimated parameters. We encountered this problem only in a few occasions and always in voxels close to large vessels or at the periphery of the brain where signal variability may be high because of poor SNR and local misregistration. In such rare cases, prior information inferred from neighboring voxels may be used to guide the iterative reweighting process in the right direction. Alternatively, these voxels can be masked out by setting a threshold of acceptance for the χ^2 of the final fit.

CONCLUSION

Both our Monte Carlo simulation and real data results show that the proposed RESTORE algorithm is an effective tool for robust estimation of the diffusion tensor in the presence of artifactual data points in the diffusion weighted images. This method eliminates the need for identifying corrupted images by visual inspection and also automatically detects spatially localized outliers that would be easily missed at visual inspection. We believe that this approach would be particularly useful for routine processing of clinical DT-MRI data. Its ability to provide an objective and operator-independent exclusion of artifactual data points would also be a desirable feature for multicenter research studies.

REFERENCES

1. Mattiello J, Basser PJ, Le Bihan D. The b matrix in diffusion tensor echo-planar imaging. Magn Reson Med 1997;37:292–300.
2. Basser PJ, Mattiello J, LeBihan D. Estimation of the effective self-diffusion tensor from the NMR spin echo. J Magn Reson B 1994;103: 247–254.
3. Henkelman RM. Measurement of signal intensities in the presence of noise in MR images. Med Phys 1985;12:232–233.
4. Mangin JF, Poupon C, Clark C, Le Bihan D, Bloch I. Distortion correction and robust tensor estimation for MR diffusion imaging. Med Image Anal 2002;6:191–198.
5. Geman S, McClure DE. Statistical methods for tomographic image reconstruction. Bull Int Stat Inst 1987;52:5–21.
6. Hampel F. The influence curve and its role in robust estimation. J Am Stat Assoc 1974;69:383–393.
7. Rousseuw PJ, Croux C. Alternatives to the median absolute deviation. J Am Stat Assoc 1993;88:1273–1283.
8. Markwardt CB. MPFIT: IDL curve fitting and function optimization. http://astrogphysicswiscedu/~craigm/idl/fittinghtml.
9. Bevington P. Data reduction and error analysis for the physical sciences. McGraw–Hill: New York; 1969.
10. Pierpaoli C, Jezzard P, Basser PJ, Barnett A, Di Chiro G. Diffusion tensor MR imaging of the human brain. Radiology 1996;201:637–648.
11. Davis T, Wedeen V, Weisskooff R, Rosen B. White matter tract visualization by echo-planar MRI. In: Proceedings of the 12th Annual Meeting of SMRM, New York, 1993:289.
12. Jones DK. The effect of gradient sampling schemes on measures derived from diffusion tensor MRI: a Monte Carlo study. Magn Reson Med 2004;51:807–815.
13. Jones DK, Horsfield MA, Simmons A. Optimal strategies for measuring diffusion in anisotropic systems by magnetic resonance imaging. Magn Reson Med 1999;42:515–525.
14. Basser PJ, Pierpaoli C. Microstructural and physiological features of tissues elucidated by quantitative-diffusion-tensor MRI. J Magn Reson B 1996;111:209–219.
15. Pierpaoli C, Marenco S, Rohde G, Jones D, Barnett A. Analyzing the contribution of cardiac pulsation to the variability of quantities derived from the diffusion tensor. In: Proceedings of the 11th Annual Meeting of ISMRM, Toronto, Canada, 2003. p 70.
16. Rohde GK, Barnett AS, Basser PJ, Marenco S, Pierpaoli C. Comprehensive approach for correction of motion and distortion in diffusion-weighted MRI. Magn Reson Med 2004;51:103–114.
17. Pierpaoli C, Basser PJ. Toward a quantitative assessment of diffusion anisotropy. Magn Reson Med 1996;36:893–906.
18. Huber P. Robust statistics. New York: Wiley; 1981.
19. Meer P, Mintz D, Rosenfeld A, Kim DY. Robust regression methods for computer vision: a review. Int J Comput Vis 1991;6:59–70.
20. Wheeler-Kingshott CAM, Boulby PA, Symms M, Barker GJ. Optimised cardiac gating for high-resolution whole brain DTI on a standard scanner. In: Proceedings of the 10th Annual Meeting of ISMRM, Honolulu, 2002. p 1118.